Article

Competitive Na and Rb Binding in the Minor Groove of DNA

Flaminia Cesare Marincola, Vladimir P. Denisov, and Bertil Halle

J. Am. Chem. Soc., **2004**, 126 (21), 6739-6750• DOI: 10.1021/ja049930z • Publication Date (Web): 06 May 2004

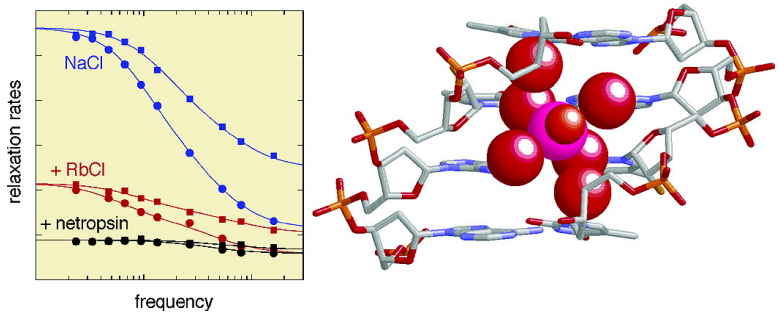

More About This Article

Additional resources and features associated with this article are available within the HTML version:

- Supporting Information
- Links to the 9 articles that cite this article, as of the time of this article download
- Access to high resolution figures
- Links to articles and content related to this article
- Copyright permission to reproduce figures and/or text from this article

View the Full Text HTML

J|A|C|S
ARTICLES
Published on Web 05/06/2004

Competitive Na^+ and Rb^+ Binding in the Minor Groove of DNA

Flaminia Cesare Marincola,† Vladimir P. Denisov, and Bertil Halle*

Contribution from the Department of Biophysical Chemistry, Lund University, SE-22100 Lund, Sweden

Received January 5, 2004; E-mail: bertil.halle@bpc.lu.se

Abstract: Sequence-dependent coordination of alkali ions to the nucleotide bases in the minor groove of AT-tract *B*-DNA has recently been inferred from X-ray crystallography, solution NMR and computer simulations. Here, we present new ^{23}Na and ^{87}Rb magnetic relaxation dispersion (MRD) data that demonstrate competitive and long-lived binding of Na^+ and Rb^+ ions in the minor groove of the *B*-DNA duplex $[d(CGCGAATTCGCG)]_2$. The Na^+/Rb^+ selectivity of the minor groove is found to be weak, consistent with local structural flexibility. The ion occupancies derived from the MRD data are substantially higher than previously reported, suggesting that groove-bound ions significantly influence the energetics and structural polymorphism of DNA in vivo. For example, in the presence of 0.20 M Na^+ and 0.56 M Rb^+ at 4 °C, the ApT site in the minor groove is occupied by a Rb^+ ion, a Na^+ ion, or a water molecule 40, 10, and 50% of the time, respectively. In the absence of Rb^+, the Na^+ occupancy increases to 50%. At 4 °C, the mean residence time of groove-bound ions is 0.2 ± 0.1 μs for Rb^+ and 10 ns to 100 μs for Na^+. A shorter correlation time of 2 ns is attributed to counterions bridging cross-strand phosphate groups.

1. Introduction

Compelling evidence for sequence-dependent intrusion of monovalent, partly dehydrated cations into the minor groove of *B*-form DNA has come from X-ray crystallography,[1−6] solution NMR,[7,8] and molecular dynamics simulations.[9−14] These findings have received considerable attention,[15−17] not least because intimate ion association could play a role in sequence-dependent variations of DNA structure.[18,19] While it has been firmly established that monovalent cations can be directly coordinated to the nucleotide bases in the narrowed minor groove of AT-tracts in *B*-DNA duplexes, we are still far from a quantitative understanding of such specific ion−DNA interactions under physiologically relevant solution conditions.

Much of the experimental evidence for monovalent cation penetration of the minor groove has been obtained by X-ray diffraction. Because of the difficulty of distinguishing Na^+ or K^+ ions from water molecules in the electron density map,[20] there has been some disagreement over interpretations.[21−23] Partially occupied ion sites have thus been reliably detected only for the heavier cations Rb^+,[4] Cs^+,[5] and Tl^+.[6] Even in these cases, the unknown ionic composition of the solvent medium (which usually includes Mg^{2+} ions) prevents quantitative comparisons with solution studies. Another complication is that all these crystal structures have been determined at cryogenic temperatures, some 150−200 K below the physiological range. The relevance of such structures relies on the unproven assumption that flash-cooling is sufficiently fast to kinetically trap the room-temperature structure. This widespread assumption has recently been challenged by calculations showing that solvent-coupled degrees of freedom are quenched near 200 K and thus represent the equilibrium at that temperature.[24] Ion binding in the minor groove is a prime candidate for such cryoartifacts, since the ion exchange rate (as determined here) is some 5 orders of magnitude higher than the typical cooling rate.

† Present address: Dipartimento di Scienze Chimiche, Cittadella Universitaria di Monserrato, I-09042 Monserrato (CA), Italy.

(1) Bartenev, V. N.; Golovamov, Eu. I.; Kapitonova, K. A.; Mokulskii, M. A.; Volkova, L. I.; Skuratovskii, I. Ya. *J. Mol. Biol.* **1983**, *169*, 217−234.
(2) Shui, X.; Sines, C. C.; McFail-Isom, L.; VanDerveer, D.; Williams, L. D. *Biochemistry* **1998**, *37*, 16 877−16 887.
(3) Shui, X.; McFail-Isom, L.; Hu, G. G.; Williams, L. D. *Biochemistry* **1998**, *37*, 8341−8355.
(4) Tereshko, V.; Minasov, G.; Egli, M. *J. Am. Chem. Soc.* **1999**, *121*, 3590−3595.
(5) Woods, K. K.; McFail-Isom, L.; Sines, C. C.; Howerton, S. B.; Stephens, R. K.; Williams, L. D. *J. Am. Chem. Soc.* **2000**, *122*, 1546−1547.
(6) Howerton, S. B.; Sines, C. C.; VanDerveer, D.; Williams, L. D. *Biochemistry* **2001**, *40*, 10 023−10 031.
(7) Hud, N. V.; Sklenár, V.; Feigon, J. *J. Mol. Biol.* **1999**, *286*, 651−660.
(8) Denisov, V. P.; Halle, B. *Proc. Natl. Acad. Sci. U.S.A.* **2000**, *97*, 629−633.
(9) Young, M. A.; Jayaram, B.; Beveridge, D. L. *J. Am. Chem. Soc.* **1997**, *119*, 59−69.
(10) Feig, M.; Pettitt, B. M. *J. Mol. Biol.* **1999**, *286*, 1075−1095.
(11) McConnell, K. J.; Beveridge, D. L. *J. Mol. Biol.* **2000**, *304*, 803−820.
(12) Hamelberg, D.; McFail-Isom, L.; Williams, L. D.; Wilson, W. D. *J. Am. Chem. Soc.* **2000**, *122*, 10 513−10 520.
(13) Stefl, R.; Koca, J. *J. Am. Chem. Soc.* **2000**, *122*, 5025−5033.
(14) Mocci, F.; Saba, G. *Biopolymers* **2003**, *68*, 471−485.
(15) McFail-Isom, L.; Sines, C. C.; Williams, L. D. *Curr. Opin. Struct. Biol.* **1999**, *9*, 298−304.
(16) Hud, N. V.; Polak, M. *Curr. Opin. Struct. Biol.* **2001**, *11*, 293−301.
(17) Egli, M. *Chem. Biol.* **2002**, *9*, 277−286.
(18) Rouzina, I.; Bloomfield, V. A. *Biophys. J.* **1998**, *74*, 3152−3164.
(19) Williams, L. D.; Maher, L. J. *Annu. Rev. Biophys. Biomol. Struct.* **2000**, *29*, 497−521.
(20) Tereshko, V.; Wilds, C. J.; Minasov, G.; Prakash, T. P.; Maier, M. A.; Howard, A.; Wawrzak, Z.; Manoharan, M.; Egli, M. *Nucl. Acids Res.* **2001**, *29*, 1208−1215.
(21) Chiu, T. K.; Kaczor-Grzeskowiak, M.; Dickerson, R. E. *J. Mol. Biol.* **1999**, *292*, 589−608.
(22) Tereshko, V.; Minasov, G.; Egli, M.*J. Am. Chem. Soc.* **1999**, *121*, 470−471.
(23) Johansson, E.; Parkinson, G.; Neidle, S. *J. Mol. Biol.* **2000**, *300*, 551−561.
(24) Halle, B. *Proc. Natl. Acad. Sci. U.S.A.* **2004**, *101*, 4793−4798.

For these reasons, it is important to complement crystallographic analysis with studies by solution techniques, such as NMR. Although alkali ions cannot be studied directly by high-resolution NMR, sequence-specific binding of ammonium ions has been demonstrated through the observation of intermolecular $^1H-^1H$ cross-relaxation with adenine H2 protons in the minor groove AT-tract of several oligonucleotide duplexes.[7,25] In the case of Na^+, indirect evidence of minor-groove intrusion has been provided by capillary electrophoresis experiments.[26] Molecular dynamics simulations have also shown that Na^+ ions can replace water molecules in the primary solvation layer in the minor groove of AT-tract *B*-DNA.[9−14]

Magnetic relaxation dispersion (MRD) is arguably the most direct experimental method for determining the extent and kinetics of specific alkali ion binding, as well as hydration, of DNA in aqueous solution.[27,28] In a previous ^{23}Na MRD study,[8] long-lived (residence time > 10 ns) Na^+ binding to *B*-DNA dodecamers was demonstrated and shown to correlate with the length of the AT-tract. Moreover, the long-lived Na^+ binding was found to be virtually eliminated by netropsin binding, thus establishing the AT-tract as the location of the specific ion binding sites.[8] Ion competition experiments were also reported, albeit at a single frequency, indicating that heavier alkali ions and ammonium ions bind with similar or somewhat higher affinity than Na^+.[8] However, the interpretation of these competition experiments is not straightforward (M. Guéron, personal communication). Without direct MRD measurements on the competing ion, it is difficult to exclude the possibility that Na^+ ions are depleted from the minor groove simply because of the statistical dilution of Na^+ ions near the DNA surface.

The present work is only concerned with the dodecamer $[d(CGCGAATTCGCG)]_2$, but extends the previous MRD study in several respects. Because the previous study indicated a rather low Na^+ occupancy, corresponding roughly to one bound Na^+ ion per 40 DNA strands, depurination or truncated sequences might have affected the results. We now use a DNA preparation of very high purity, studied at 5-fold lower concentration. Furthermore, we have now measured the full ^{23}Na and ^{87}Rb MRD profiles in a DNA solution containing both ions, with and without added netropsin. In this way, we could establish that both ions bind to the same site in the minor groove. Third, we have carried out more extensive calculations of the electric field gradient experienced by bound ions. We thus find that the quadrupole coupling constant is significantly smaller than previously thought. As a result, the ion occupancies deduced from the MRD data are considerable higher than previously reported, suggesting that groove-bound ions may, indeed, be a significant factor in the structural polymorphism of DNA.

2. Materials and Methods

2.1. Sample Preparation. The sodium salt of the DNA dodecamer d(CGCGAATTCGCG) (abbreviated A_2T_2) was obtained from Oligos Etc. (Wilsonville, OR). The purity was checked by analytical ion-exchange HPLC (Scandinavian Gene Synthesis, Köping, Sweden), yielding 97% full-length oligomer. Crystalline netropsin (purity > 98%) was obtained from Boehringer Mannheim. Inorganic salts were of analytical grade.

The dodecamer solution was prepared at a duplex concentration of 1.47 mM by dissolving a known amount of dry A_2T_2 in D_2O (99.9 atom % ^2H, low paramagnetic content) from Cambridge Isotope Laboratories (Andover, MA). The molar concentration was calculated with a duplex molar mass of 2×3888 g mol^{-1}. The sample was annealed by slow cooling (60 min) from 75 °C to room temperature. Solution pH (not corrected for isotope effects) was adjusted to 7.02 ± 0.02. No buffer was added. Dry NaCl, RbCl, and crystalline netropsin were added to the solution, yielding Na^+ and Rb^+ concentrations of 0.20 and 0.56 M, respectively, and a netropsin/duplex mole ratio of 1.1 ± 0.1. The quoted DNA and salt concentrations are accurate to better than 3%.

2.2. ^{23}Na and ^{87}Rb MRD Experiments. Longitudinal and transverse ^{23}Na and ^{87}Rb relaxation rates were measured as previously described,[8] using five NMR spectrometers operating in the magnetic field range 0.2−14.1 T. For ^{87}Rb, each relaxation experiment comprised 25−40 variable-delay spectra with a signal-to-noise ratio of 60−100, requiring accumulation of up to 2×10^5 transients per spectrum. The temperature of the MRD sample (ca. 0.9 mL in a 10-mm tube) was maintained at 4.0 ± 0.1 °C using a thermostated air flow and a copper−constantan thermocouple. ^{23}Na and ^{87}Rb relaxation rates in bulk 0.2 M NaCl and 0.5 M RbCl D_2O solutions were measured at several magnetic fields, yielding $R_{bulk}(^{23}Na) = 34.6 \pm 0.2$ s^{-1} and $R_{bulk}(^{87}Rb) = 746 \pm 5$ s^{-1} at 4 °C. Because R_{bulk} does not depend on the magnetic field strength, these reference measurements also served as an additional temperature check.

2.3. ^{31}P Relaxation Experiments. To obtain an independent estimate of the DNA tumbling time, τ_R, we measured the ^{31}P relaxation rates at 4 °C in the mixed-salt MRD sample (transferred to a 5-mm tube) using Varian INOVA 500 and 600 spectrometers. Due to broadening of the 11 ^{31}P peaks of A_2T_2, only two overlapping peaks could be resolved below 10 °C, with the minor upfield peak assigned to the central four phosphates.[29] The longitudinal and transverse ^{31}P relaxation rates were obtained from exponential fits to the total integrated intensity of the two peaks in inversion−recovery or spin−echo experiments with a 90° pulse width of 20 μs, 20 delay times, a recycling delay of 15 s, and up to 256 transients. The ^{31}P relaxation was modeled as a sum of a chemical shielding anisotropy (CSA) contribution, with parameters $\Delta\sigma = 150$ ppm and $\eta = -0.6$,[30] and a dipole−dipole contribution from a single proton at an effective distance of 2.0 Å.[31] To account for internal motions, we used a two-term spectral density function[31] with an order parameter S^2 and an internal correlation time τ_{int}. The quoted uncertainties in the three fitting parameters τ_R, S^2, and τ_{int} take into account a possible contribution from paramagnetic impurities, estimated to be < 0.1 s^{-1} for R_1 and < 10 s^{-1} for R_2. When the same analysis was performed on the individual ^{31}P peaks, similar τ_R values but smaller S^2 and τ_{int} values were obtained for the major peak (assigned to the peripheral phosphates).

2.4. Analysis of MRD Data. Being spin-3/2 quadrupolar nuclei, both ^{23}Na and ^{87}Rb exhibit biexponential longitudinal and transverse magnetic relaxation.[32] However, in DNA solutions, a biexponential magnetization decay is usually observed only for transverse relaxation at high magnetic fields and low salt concentrations.[8,33] In the present study, nearly all (99 out of 102) relaxation decays were thus monoexponential within the experimental accuracy. Under fast-exchange conditions, that is, when the residence times, τ_{res}, of bound ions are much shorter than their zero-frequency intrinsic relaxation times, $T_I(0)$, the longitudinal and transverse relaxation rates can be expressed in

(25) Feigon, J.; Butcher, S. E.; Finger, L. D.; Hud, N. V. *Methods Enzymol.* **2001**, *338*, 400−420.
(26) Stellwagen, N. C.; Magnusdottir, S.; Gelfi, C.; Righetti, P. G. *J. Mol. Biol.* **2001**, *305*, 1025−1033.
(27) Halle, B.; Denisov, V. P. *Biopolymers* **1998**, *48*, 210−233.
(28) Halle, B.; Denisov, V. P. *Methods Enzymol.* **2001**, *338*, 178−201.
(29) Ott, J.; Eckstein, F. *Biochemistry* **1985**, *24*, 2530−2535.
(30) Wu, Z.; Tjandra, N.; Bax, A. *J. Am. Chem. Soc.* **2001**, *123*, 3617−3618.
(31) Lane, A. N. *Methods Enzymol.* **1995**, *261*, 413−435.
(32) Abragam, A. *The Principles of Nuclear Magnetism*; Clarendon Press: Oxford, 1961.
(33) Nordenskiöld, L.; Chang, D. K.; Anderson, C. F.; Record, M. T. *Biochemistry* **1984**, *23*, 4309−4317.

terms of the exchange-averaged spectral density function (SDF), $J(\omega)$. From fits to monoexponential magnetization decays, one obtains the effective relaxation rates[34,35]

$$R_1^e(\omega_0) = 0.2J(\omega_0) + 0.8J(2\omega_0) \quad (1a)$$

$$R_2^e(\omega_0) = 0.3J(0) + 0.5J(\omega_0) + 0.2J(2\omega_0) \quad (1b)$$

where $\omega_0 = 2\pi\,\nu_0$ is the ^{23}Na or ^{87}Rb resonance frequency in angular frequency units. In the three cases where the transverse magnetization decay was significantly biexponential, we obtained R_2^e from the fitted rates, $R_2^+ = 0.5J(0) + 0.5J(\omega_0)$ and $R_2^- = 0.5J(\omega_0) + 0.5J(2\omega_0)$, according to $R_2^e = 0.6R_2^+ + 0.4R_2^-$.[34]

The frequency-dependent relaxation data were modeled with a SDF of the form[35]

$$J(\omega) = R_{bulk} + \alpha + \beta\frac{\tau_\beta}{1+(\omega\tau_\beta)^2} + \gamma\frac{\tau_\gamma}{1+(\omega\tau_\gamma)^2} \quad (2)$$

The physical significance of these terms is as follows.[36−39] In bulk aqueous electrolyte solutions, the quadrupolar relaxation rate, R_{bulk}, of monatomic ionic species such as Na^+ and Rb^+ is due to librations and intermolecular vibrations within the ionic hydration shell that give rise to subpicosecond fluctuations in the magnitude and orientation of the electric field gradient (EFG) tensor at the nuclear site. The frequency-independent term, α, represents the effect of perturbations of these fast fluctuations and of local ion diffusion near the DNA surface. The β term, with a correlation time, τ_β, close to the tumbling time, τ_R, of the DNA duplex, is associated with site-bound ions with a residence time, τ_{res}, exceeding τ_R. In *B*-DNA, such long-lived ions have only been found in the AT-tract of the minor groove.[8] When these sites are blocked by the minor-groove binding drug netropsin, the β dispersion disappears.[8] The γ term, with a correlation time, τ_γ, of about 2 ns at 4 °C (see below), might reflect the modulation of the residual (partially averaged by local motions) EFG by counterion diffusion around the DNA cylinder. Alternatively, τ_γ could be the residence time of ions juxtaposed between two phosphate groups at the lips of the minor groove. In the present work, we focus on the β dispersion.

The amplitude parameters α, β, and γ and the correlation times τ_β and τ_γ were determined by nonlinear least-squares fits, using an in-house implementation of the Levenberg−Marquardt algorithm,[40] of the model defined by eqs 1 and 2 to each set of combined $R_1^e(\nu_0)$ and $R_2^e(\nu_0)$ data. The quoted uncertainties in parameter values correspond to one standard deviation and are based on fits to 1000 Monte Carlo generated data sets subject to random Gaussian noise with a standard deviation corresponding to the estimated experimental uncertainty in R_1^e and R_2^e (0.5−2% for ^{23}Na, 1−5% for ^{87}Rb). Since several of the experimental frequencies differ by a factor 2, model-independent SDF values at discrete frequencies can be extracted, either by solving the system of linear equations obtained from eq 1, or by performing a global fit to the full set of relaxation decays.[8] For the present ^{23}Na data, these procedures yield SDF values consistent (within the experimental accuracy) with the results of fits to the SDF model in eq 2.

In ^{2}H and ^{17}O MRD studies of biomolecular hydration, the analysis is usually based exclusively on the R_1 dispersion, since R_2 often contains, besides quadrupolar relaxation, interfering contributions due to hydrogen-exchange modulated spin couplings.[35] Depending on the accuracy of the data and the values of the correlation times, it may be difficult to uniquely determine a bi-Lorentzian dispersion from R_1 data spanning two frequency decades. In the present study, however, we simultaneously fit the R_1 and R_2 dispersions. Because R_2 probes the spectral density at zero frequency (see eq 1b), the β dispersion is well-defined even if the relaxation data do not extend to the low-frequency plateau.

For ^{87}Rb, an estimate of the zero-frequency intrinsic relaxation time, $T_I(0)$, indicates that the minor-groove bound ions are not in the fast-exchange limit (see below). In general, the magnetization of a spin-3/2 nucleus in two-state exchange decays as a sum of four exponentials.[41] However, under the conditions of the present study, the effective relaxation rates are given, to an excellent approximation, by eqs 1 and 2 even outside the fast-exchange regime, provided that the parameters of the β dispersion are renormalized.[35,42] Because β is proportional to the fraction, f, of groove-bound ions, we may write $\beta = fb$. The generalized expression for R_1^e is obtained by inserting into eq 1a the SDF given by eq 2 with the substitutions

$$b \rightarrow \frac{b}{(1+\epsilon)^{1/2}};\ \tau_\beta \rightarrow \frac{\tau_\beta}{(1+\epsilon)^{1/2}} \quad (3a)$$

In the case of R_2^e, the following substitutions should be made in $J(\omega_0)$ and $J(2\omega_0)$

$$b \rightarrow \frac{b}{(1+\epsilon)^{1/2}(1+0.3\epsilon)^{3/2}};\ \tau_\beta \rightarrow \tau_\beta\frac{(1+0.3\epsilon)^{1/2}}{(1+\epsilon)^{1/2}} \quad (3b)$$

whereas, in the $J(0)$ term

$$b\,\tau_\beta \rightarrow \frac{b\tau_\beta}{1+0.3\epsilon} \quad (3c)$$

In these expressions, $\epsilon = b\tau_\beta\tau_{res}$. In its generalized form, the β dispersion is thus described by three parameters: $\beta = fb, \tau_\beta$ and $b\tau_{res}$. Outside the fast-exchange regime, the residence time, τ_{res}, can therefore be determined from a joint fit to longitudinal and transverse relaxation data.

2.5. Field Gradient Calculations. For a spin-3/2 nucleus, the parameter b is related to the nuclear quadrupole coupling constant (QCC), χ, as[32,34]

$$b = \frac{2\pi^2}{5}\chi^2 \quad (4)$$

For a monatomic ion, the QCC can be expressed as[32,43]

$$\chi = \frac{eQ}{h}(1+\gamma_\infty)\left\{\langle V_{ZZ}^2\rangle + \frac{1}{3}[\langle V_{XX}^2\rangle - \langle V_{YY}^2\rangle]\right\}^{1/2} \quad (5)$$

where e is the elementary charge and h is Planck's constant. The nuclear electric quadrupole moment, Q, is 0.104 barn for ^{23}Na and 0.134 barn for ^{87}Rb.[44] The Sternheimer factor, γ_∞, which describes the effect of electronic polarization in the ion by the external charge distribution, is not as accurately known as Q. The best available values, for ions in a crystal lattice, are 5.4 for Na^+ and 53 for Rb^+.[45,46] We estimate that these values are accurate to about 5%. With these values, the ratio of the ^{87}Rb and ^{23}Na QCCs is 10.9, provided that the ions experience the same electric field gradient.

(34) Braunlin, W. H. *Adv. Biophys. Chem.* **1995**, *5*, 89−139.
(35) Halle, B.; Denisov, V. P.; Venu, K. In *Biological Magnetic Resonance*; Krishna, N. R., Berliner, L. J., Eds.; Kluwer/Plenum: New York, 1999; pp 419−484.
(36) Halle, B.; Wennerström, H.; Piculell, L. *J. Phys. Chem.* **1984**, *88*, 2482−2494.
(37) Furó, I.; Halle, B.; Quist, P.-O.; Wong, T. C. *J. Phys. Chem.* **1990**, *94*, 2600−2613.
(38) Quist, P.-O.; Halle, B.; Furó, I. *J. Chem. Phys.* **1991**, *95*, 6945−6961.
(39) Huang Kenéz, P.; Carlström, G.; Furó, I.; Halle, B. *J. Phys. Chem.* **1992**, *96*, 9524−9531.
(40) Press, W. H.; Teukolsky, S. A.; Vetterling, W. T.; Flannery, B. P. *Numerical Recipes in C*, 2nd Ed.; Cambridge University Press: Cambridge, 1992.
(41) Bull, T. E. *J. Magn. Reson.* **1972**, *8*, 344−353.
(42) Gottschalk, M.; Dencher, N. A.; Halle, B. *J. Mol. Biol.* **2001**, *311*, 605−621.
(43) Linse, P.; Halle, B. *Mol. Phys.* **1989**, *67*, 537−573.
(44) Pyykkö, P. *Mol. Phys.* **2001**, *99*, 1617−1629.
(45) Schmidt, P. C.; Sen, K. D.; Das, T. P.; Weiss, A. *Phys. Rev. B* **1980**, *22*, 4167−4179.
(46) Klösters, G.; Jansen, M. *Solid State NMR* **2000**, *16*, 279−283.

In eq 5, V_{XX}, V_{YY}, and V_{ZZ} are the principal components of the EFG tensor at the position of the ^{23}Na or ^{87}Rb nucleus and the angular brackets signify averaging over molecular motions on time scales shorter than the correlation time τ_β of the bound ions. For a distribution of classical point charges q_k at locations $\boldsymbol{r}_k$, the EFG tensor at the position $\boldsymbol{R}$ of the nucleus is given by

$$\mathbf{V}(\boldsymbol{R}) = \frac{1}{4\pi\epsilon_0}\sum_k \frac{q_k}{|\boldsymbol{R}-\boldsymbol{r}_k|^5}[3(\boldsymbol{R}-\boldsymbol{r}_k)(\boldsymbol{R}-\boldsymbol{r}_k) - |\boldsymbol{R}-\boldsymbol{r}_k|^2\,\mathbf{U}] \quad (6)$$

where ϵ_0 is the permittivity of free space and **U** is the unit tensor.

The EFG tensor for minor-groove-bound ions was computed at or near several solvent (ion or water-oxygen) sites at the floor of the minor-groove AT-tract, with the atomic coordinates taken from either of three ultrahigh-resolution (1.1−1.2 Å) crystal structures of the A_2T_2 dodecamer.[4,22,47] Hydrogen atoms were added to the structures with standard geometry for DNA and with the water geometry as in the simple point charge (SPC) model. The O−H bonds of water molecules in the primary and secondary hydration layers in the minor groove were oriented in-plane and symmetrical with respect to the H-bond acceptors. However, the two secondary-layer water molecules coordinating the ion were rotated 180° about the other H-bond so that the hydrogen points away from the ion. All other water molecules were randomly oriented. Partial atomic charges were assigned to DNA atoms according to the AMBER94 or CHARMM27 force fields, and to water atoms according to the SPC model (−0.82 on O, +0.41 on H).

2.6. Description of Competitive Ion Binding. The amplitude parameter β deduced from the MRD profiles is proportional to the fraction site-bound ions, which can be expressed as

$$f_S = \frac{\xi_S C_{DNA}}{C_S} \quad (7)$$

where the ionic species, S, is Na or Rb. Here, C_S and C_{DNA} are the total concentrations of S-ions and of duplex DNA, and ξ_S is the S-ion occupancy, that is, the mean number of site-bound S-ions per duplex. By invoking the law of mass action, the occupancy can be expressed in terms of binding constants. If S = Na is the only ionic species present that can bind to the sites considered (this condition is indicated by a superscript zero)

$$\xi^0_{Na} = \frac{K_{Na}[Na^+]}{1 + K_{Na}[Na^+]} \quad (8)$$

Because the free energy change on ion binding includes a contribution from long-range Coulomb interactions, the stoichiometric binding constant K_{Na} is not strictly independent of C_{Na} and C_{DNA}. The physical significance of K_{Na} and of the ion concentration $[Na^+]$ depend on how this complication is handled. In what might be termed a local binding model (LBM), the effects of long-range interactions are ignored and $[Na^+]$ is interpreted as the total concentration of free (not site-bound) Na^+ ions, that is, $[Na^+] = (1 - f_{Na})\,C_{Na}$. If $C_{Na} \gg C_{DNA}$, as in the present study, we have simply $[Na^+] = C_{Na}$. In the more realistic polyelectrolyte model (PEM),[48−55] one attempts to correct for long-range electrostatic ion−DNA interactions by interpreting $[Na^+]$ as the Na^+ ion concentration, $[Na^+]_0$, near the surface of the DNA duplex. In the simplest form of the PEM, one assumes that $[Na^+]_0$ is constant, independent of C_{Na} and C_{DNA}. This assumption is supported by nonlinear Poisson−Boltzmann calculations, computer simulations, and experiments.[48−56]

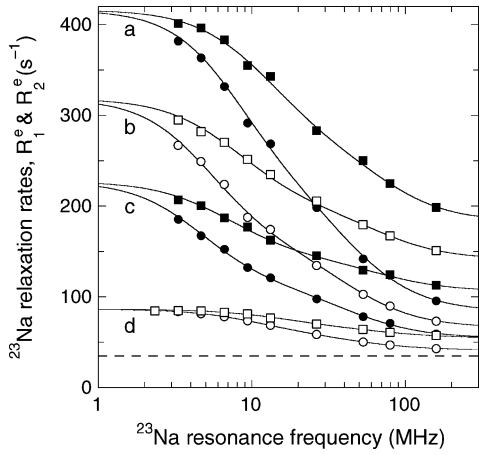

Figure 1. ^{23}Na R_1^e (circles) and R_2^e (squares) dispersions at 4.0 °C and pH 7.0 from D_2O solutions of the A_2T_2 dodecamer at different Na^+ and DNA duplex concentrations: (**a**) C_{Na} = 0.18 M, C_{DNA} = 8.2 mM; (**b**) C_{Na} = 0.34 M, C_{DNA} = 8.2 mM; (**c**) C_{Na} = 0.74 M, C_{DNA} = 8.2 mM; (**d**) C_{Na} = 0.20 M, C_{DNA} = 1.5 mM. The dispersion curves resulted from bi-Lorentzian fits according to eqs 1 and 2, with the parameter values given in Table 1. The uncertainty in R_1^e and R_2^e is comparable to the size of the data symbols. The dashed line represents the ^{23}Na relaxation rate, R_{bulk}, in a bulk 0.2 M NaCl D_2O solution at 4.0 °C.

In the presence of a second ionic species (Rb^+ in the present study) that competes for the same binding site (we assume that there is only one binding site per duplex), the ion occupancies are linked by

$$\frac{\xi_{Na}}{1 - \xi_{Na} - \xi_{Rb}} = K_{Na}[Na^+] \quad (9)$$

and a similar relation with Na and Rb interchanged. In the simplest version of the PEM, one assumes that the total ion concentration at the surface is constant, $[Na^+]_0 + [Rb^+]_0 = C_0$, and that the ionic composition at the surface is purely statistical, $[Na^+]_0/[Rb^+]_0 = C_{Na}/C_{Rb}$. We refer to this model as the restricted PEM (RPEM). It then follows that, for both models

$$\frac{\xi_{Na}}{\xi_{Rb}} = \frac{K_{Na}C_{Na}}{K_{Rb}C_{Rb}} \quad (10)$$

and

$$\xi_{Na} = \frac{\xi^0_{Na}}{1 + \lambda C_{Rb}/C_{Na}} \quad (11)$$

However, the significance of the coefficient λ is different in the two models

$$\lambda = \begin{cases} \dfrac{\xi^0_{Na}}{\xi_{Na}}\dfrac{K_{Rb}}{K_{Na}} & \text{(LBM)} \\ 1 + \xi^0_{Na}\left(\dfrac{K_{Rb}}{K_{Na}} - 1\right) & \text{(RPEM)} \end{cases} \quad (12)$$

3. Results

3.1. ^{23}Na and ^{87}Rb MRD Profiles from DNA Solutions. Figure 1 shows the ^{23}Na R_1^e and R_2^e dispersions measured at 4.0

(47) Sines, C. C.; McFail-Isom, L.; Howerton, S. B.; VanDerveer, D.; Williams, L. D. *J. Am. Chem. Soc.* **2000**, *122*, 11 048−11 056.
(48) Fuoss, R. M.; Katchalsky, A.; Lifson, S. *Proc. Natl. Acad. Sci. U.S.A.* **1951**, *37*, 579−589.
(49) Alfrey, T. J.; Berg, P. W.; Morawetz, H. *Polymer Sci.* **1951**, *37*, 579−589.
(50) Oosawa, F. *Polyelectrolytes*; M. Dekker: New York, 1971.
(51) Manning, G. S. *Quart. Rev. Biophys.* **1978**, *11*, 179−246.
(52) Weisbuch, G.; Guéron, M. *Biopolymers* **1980**, *19*, 353−382.
(53) Guéron, M.; Weisbuch, G. *J. Phys. Chem.* **1981**, *85*, 517−525.
(54) Guéron, M.; Weisbuch, G. *Biochimie* **1981**, *63*, 821−825.
(55) Anderson, C. F.; Record, M. T. *Annu. Rev. Phys. Chem.* **1995**, *46*, 657−700.
(56) Das, R.; Mills, T. T.; Kwok, L. W.; Maskel, G. S.; Millett, I. S.; Doniach, S.; Finkelstein, K. D.; Herschlag, D.; Pollack, L. *Phys. Rev. Lett.* **2003**, *90*, 188 103.

Table 1. Results of Fits to ^{23}Na and ^{87}Rb MRD Data[a]

nucleus	T (°C)	C_{DNA}[b] (mM)	C_{Na}[c] (M)	C_{Rb}[c] (M)	α (s^{-1})	β (10^9 s^{-2})	τ_β (ns)	γ (10^9 s^{-2})	τ_γ (ns)
^{23}Na	4.0	8.2	0.18	0	50 ± 3	19 ± 3	11 ± 1	64 ± 4	2.0 ± 0.2
^{23}Na	4.0	8.2	0.34	0	32 ± 2	10 ± 1	16 ± 1	41 ± 2	2.1 ± 0.2
^{23}Na	4.0	8.2	0.74	0	20 ± 1	6.4 ± 0.4	18 ± 1	27 ± 1	2.0 ± 0.2
^{23}Na	27.0	1.47	0.20	0	3.7 ± 0.6	1.5 ± 0.5	3.7[d]	7.7 ± 1.0	1.4 ± 0.3
^{23}Na	4.0	1.47	0.20	0	6.8 ± 0.4	3.6 ± 0.4	8.0 ± 0.5	8.7 ± 0.6	1.8 ± 0.2
^{23}Na	4.0	1.47	0.20	0.56	1.1 ± 0.3	0.6 ± 0.1	14 ± 2	3.7 ± 0.4	1.9 ± 0.3
^{23}Na	4.0	1.47 + net[e]	0.20	0.56	1.2 ± 0.2			1.2 ± 0.3	2.4 ± 0.4
^{87}Rb	4.0	1.47	0.20	0.56	92 ± 16	126 ± 50	18 ± 4	215 ± 30	2.6 ± 0.7
^{87}Rb	4.0	1.47 + net[e]	0.20	0.56	47 ± 6			157 ± 10	2.0 ± 0.1

[a] All data sets were fitted with the fast-exchange model, except the ^{87}Rb data without netropsin, where $\tau_{res} = 0.2 \pm 0.1$ μs was obtained. [b] Duplex concentration. Data at 8.2 mM were taken from ref 8; other data are from the present work. [c] Total concentration of the indicated ion. The first entry refers to sodium DNA without added salt; hence $C_{Na} = 8.2 \times 22 = 180$ mM. [d] The τ_β value was η/T scaled from 4 °C and held fixed in the fit. [e] AT-tract of minor groove blocked by 1.1 mol netropsin per mol duplex.

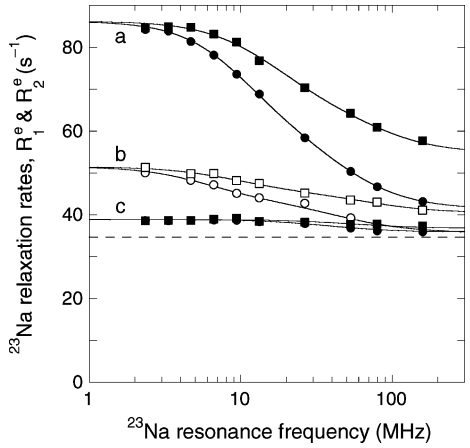

Figure 2. ^{23}Na R_1^e (circles) and R_2^e (squares) dispersions at 4.0 °C and pH 7.0 from 1.5 mM D_2O solutions of the A_2T_2 duplex with 0.20 M Na^+ (**a**) before and (**b**) after addition of 0.56 M RbCl and (**c**) after the subsequent addition of 1.1 mol netropsin per mol duplex. Data set (a) corresponds to data set (d) in Figure 1. The dispersion curves resulted from bi-Lorentzian (a and b) or mono-Lorentzian (c) fits according to eqs 1 and 2, with the parameter values given in Table 1. The uncertainty in R_1^e and R_2^e is comparable to the size of the data symbols. The dashed line represents the ^{23}Na relaxation rate, R_{bulk}, in a bulk 0.2 M NaCl D_2O solution at 4.0 °C.

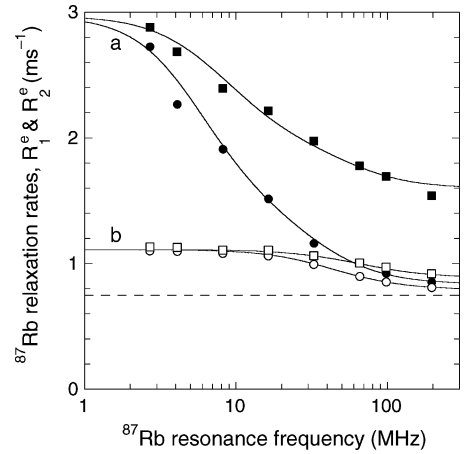

Figure 3. ^{87}Rb R_1^e (circles) and R_2^e (squares) dispersions at 4.0 °C and pH 7.0 from 1.5 mM D_2O solutions of the A_2T_2 duplex with 0.20 M Na^+ and 0.56 M Rb^+ (**a**) before and (**b**) after addition of 1.1 mol netropsin per mol duplex. These ^{87}Rb dispersions were obtained from the same samples as the ^{23}Na dispersions (b) and (c) in Figure 2. The dispersion curves resulted from bi-Lorentzian (a) or mono-Lorentzian (b) fits according to eqs 1 and 2 (and eq 3 for dispersion a), with the parameter values given in Table 1. The dashed line represents the ^{87}Rb relaxation rate, R_{bulk}, in a bulk 0.5 M RbCl D_2O solution at 4.0 °C.

°C from D_2O solutions of the A_2T_2 dodecamer at different duplex and NaCl concentrations. Three of these dispersions are from an earlier study[8] with less highly purified A_2T_2 at 5-fold higher concentration as compared to the present work. Nevertheless, the results of the two studies are mutually consistent (see below). All of the ^{23}Na dispersions in Figure 1 are well described by the bi-Lorentzian SDF in eq 2. If only one Lorentzian term is included, the χ^2 merit function increases by an order of magnitude. The parameter values resulting from the fits are collected in Table 1.

By studying the effect on the ^{23}Na dispersion of varying the nucleotide base sequence and of blocking the minor groove by netropsin, it has previously been demonstrated that the β dispersion is produced by long-lived Na^+ ions residing in the AT-tract of the minor groove.[8] The quantitative analysis of the present results (see below) supports this conclusion, but indicates a higher binding affinity. This analysis is based on five new data sets: ^{23}Na dispersions for A_2T_2 in NaCl and after successive additions of RbCl and netropsin, and ^{87}Rb dispersions on the last two samples.

Upon addition of 0.56 M RbCl, the ^{23}Na relaxation rates are reduced at all investigated frequencies (Figure 2). In particular, the β dispersion now has a much smaller amplitude (cf. the β parameters in Table 1). This indicates that most of the long-lived Na^+ ions are displaced from the minor groove. The β dispersion disappears completely after addition of 1.1 equivalent of netropsin, which is known to bind in the A_2T_2 tract of the minor groove.[57,58] This confirms previous ^{23}Na MRD results,[8] showing that the long-lived ions reside in this location.

The suppression of the β dispersion on addition of RbCl is in line with the previously reported effects of several different competing counterions.[8] The previous results were based on measurements of $R_2^e - R_1^e$ at a single high ^{23}Na frequency, where this difference is dominated by $J(0)$. To determine the effect of the competing ion on the β dispersion, it is necessary to record the full ^{23}Na dispersion in the mixed salt solution, as in Figure 2. Even with this more detailed information, it is difficult to establish if the suppression of the β dispersion is due to displacement of Na^+ ions in the minor groove by Rb^+ ions or by water molecules. To remove this ambiguity, we recorded the ^{87}Rb dispersion from the same sample as was used for the ^{23}Na dispersion. The observation of a pronounced ^{87}Rb β dispersion (Figure 3) provides conclusive evidence for long-lived Rb^+ binding. Furthermore, the complete loss of the β dispersion on addition of netropsin (Figure 3) shows that the

(57) Patel, D. J. *Proc. Natl. Acad. Sci. U.S.A.* **1982**, *79*, 6424−6428.
(58) Goodsell, D. S.; Kopka, M. L.; Dickerson, R. E. *Biochemistry* **1995**, *34*, 4983−4993.

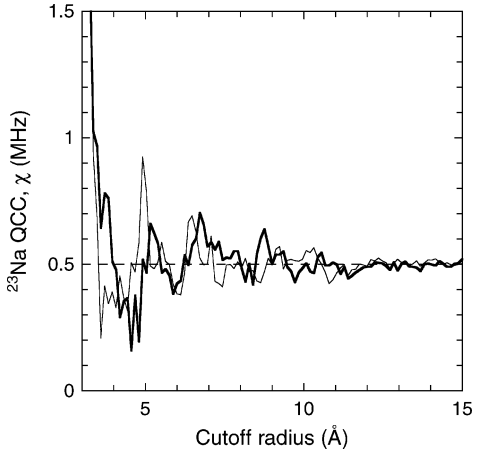

Figure 4. ^{23}Na quadrupole coupling constant, χ, for a Na^+ ion at the ApT site in the A_2T_2 crystal structure 460d,[4] computed with the aid of eqs 5 and 6 and partial atomic charges from the all-atom force fields AMBER94 (thick line) and CHARMM27 (thin line). Four water molecules in the primary spine and six water molecules in the secondary spine were oriented for optimal H-bonding, while the remaining 179 crystal waters were randomly oriented. The phosphate charges were set to −0.24 to mimic the effect of "condensed" counterions. The figure shows the convergence of the QCC with the cutoff radius for inclusion of partial charges. In this case, both force fields converge to the same QCC value of 0.50 MHz (dash−dotted line). The ^{87}Rb QCC for a Rb^+ ion at the same location is a factor 10.9 larger than the ^{23}Na QCC.

long-lived Rb^+ ions, like the long-lived Na^+ ions, reside in the AT-tract of the minor groove. We conclude, therefore, that Na^+ and Rb^+ ions compete directly for the same site in the minor groove of the A_2T_2 AT-tract.

3.2. QCC for Ions in the Minor Groove. To deduce the site occupancy of Na^+ or Rb^+ ions in the minor groove from our relaxation data, we need an accurate estimate of the quadrupole coupling constant (QCC) in these sites. We have therefore calculated the QCC for ions in the primary solvation layer at the floor of the minor groove using atomic coordinates from either of three ultrahigh-resolution crystal structures of the A_2T_2 dodecamer,[4,22,47] including water molecules and added hydrogen atoms. Partial atomic charges for DNA and water were taken from either of two all-atom force fields (Section 2.5). Figure 4 shows that the two force fields yield very similar results and that the EFG that governs the QCC (eq 5) is essentially determined by the charge distribution within 10 Å. To mimic the effect of the counterion atmosphere, the EFG calculations were performed with reduced phosphate charges. However, because of the relatively short range of the EFG (Figure 4), this charge renormalization has little effect on the QCC (cf. the first two rows of Table 2).

EFG calculations were performed at the site of the central water oxygen in the primary solvation layer of the minor groove (the ApT site) as well as at the sites of the two flanking water oxygens (ApA sites). If no water molecules are included in the EFG-generating charge distribution, the ^{23}Na QCC, χ, in the ApT site is about 1 MHz. Inclusion of the water molecules in the primary hydration layer (two on either side of the ApT site) has a surprisingly small effect on χ (Table 2). However, when the six central water molecules of the secondary solvation layer are added (with the two innermost water molecules oriented as expected when an ion occupies the ApT site), χ is reduced by about a factor 2 (depending on force field). Addition of the remaining ca. 200 crystal waters has a small but significant effect on χ (in opposite directions for the two force fields). However, the orientation of these external water molecules is unimportant. With all water molecules included, the two force fields give (somewhat fortuitously) the same result. On the basis of the variation found for the ApT site in three crystal structures (Table 3) as well as other considerations (Section 4.4), we estimate that $\chi(^{23}Na) = 0.5 \pm 0.2$ MHz in the ApT site. This estimate should also be adequate for the flanking ApA sites, for which the calculations yield 15−20% larger χ on average (Table 3). The χ variation between the two ApA sites and between the three crystal structures is correlated with variations in coordination geometry (Table 3). For example, the large χ value for site #115 in the structure 436d can be attributed to a short thymine O2 distance and a long secondary water distance, lowering the symmetry of the coordination shell and thus increasing the EFG. These χ variations are crystal artifacts; in solution, the A_2T_2 duplex must exhibit 2-fold symmetry on average. On the basis of the known nuclear quadrupole moments and electronic polarization factors (Section 2.5), the ^{87}Rb QCC should be a factor 10.9 larger than the ^{23}Na QCC. We thus estimate that $\chi(^{87}Rb) = 5.5 \pm 2$ MHz.

Table 2. Calculated ^{23}Na QCC in the ApT Site of the A_2T_2 Dodecamer[a]

	water molecules included			χ (MHz)[f]	
Z_P[b]	primary[c]	secondary[d]	external[e]	AMBER	CHARMM
−1.00	no	no	no	0.98	0.92
−0.24	no	no	no	1.04	0.90
−0.24	yes	no	no	0.95	0.83
−0.24	yes	yes	no	0.41	0.58
−0.24	yes	yes	yes	0.49 ± 0.02	0.51 ± 0.02

[a] EFG tensor computed at the position of the oxygen atom of the central water molecule (# 110 in the PDB file) in the crystal structure 460d.[4] [b] Phosphate net charge, renormalized by counterion "condensation". [c] Inclusion of 4 water molecules in primary solvation layer, 2 on either side of the ApT site. [d] Inclusion of 6 water molecules in secondary solvation layer, with the 2 central O−H bonds rotated away from the ion. [e] Inclusion of 179 external crystal water molecules. The 0.02 MHz standard deviation of χ is based on 100 external water configurations with orientations chosen randomly from an isotropic distribution. [f] The ^{87}Rb QCC is obtained by multiplying the ^{23}Na χ values in the Table by 10.9.

Table 3. Calculated ^{23}Na QCC in ApT and ApA Sites of Different A_2T_2 Structures[a]

	ion site[c]		coordination (Å)[d]				χ (MHz)[e]	
PDB[b]	type	#	O2	O/N	Wa	Wb	AMBER	CHARMM
460d	ApT	110	2.77	2.73	2.90	2.84	0.49	0.51
436d	ApT	110	2.74	2.74	2.91	2.80	0.39	0.52
1fq2	ApT	5	2.84	2.85	2.88	2.89	0.51	0.70
460d	ApA	104	2.85	2.83	2.75	2.81	0.62	0.82
460d	ApA	115	2.72	2.79	2.77	3.02	0.37	0.50
436d	ApA	104	2.78	2.80	2.81	2.83	0.46	0.72
436d	ApA	115	2.65	2.83	2.78	3.08	0.83	0.87
1fq2	ApA	2	2.90	2.93	2.89	2.90	0.35	0.66
1fq2	ApA	13	2.80	2.97	2.88	2.89	0.64	0.67

[a] EFG tensor computed with renormalized phosphate charges (Z_P = −0.24), four primary and six secondary water molecules in the minor groove with optimized orientations, and 170−220 randomly oriented external water molecules. [b] PDB accession code of A_2T_2 crystal structure.[4,22,47] [c] The ion is placed at the position of the oxygen atom of the indicated water molecule in the primary solvation layer. [d] Distance from ion site to the 4 nearest coordinating atoms: thymine O2, thymine O2 (ApT) or adenine N3 (ApA), and 2 water oxygens in the secondary solvation layer (Wa and Wb). [e] The quoted QCC is the mean ^{23}Na χ based on 100 external water configurations with orientations chosen randomly from an isotropic distribution. The standard deviation in χ is < 0.02 MHz in all cases. The ^{87}Rb QCC is obtained by multiplying the ^{23}Na χ values in the Table by 10.9.

4. Discussion

4.1. Ion Selectivity. The 6-fold reduction of the ^{23}Na β dispersion amplitude on addition of 0.56 M Rb^+ ions to an A_2T_2 solution containing 0.20 M Na^+ ions (Figure 2 and Table 1) suggests that Rb^+ competes with Na^+ for the binding site in the minor groove. In a previous ^{23}Na MRD study,[8] the gradual reduction of the difference $\Delta R = R_2^e - R_1^e$ at 159 MHz with increasing concentration of several monovalent counterions (including Rb^+) was also taken to indicate competition for the minor groove site. However, these interpretations are model-dependent. According to eqs 7 and 11, $\beta(^{23}Na)$ scales as $(1 + \lambda\, C_{Rb}/C_{Na})^{-1}$ on addition of Rb^+ ions. As seen from eq 12, the coefficient λ depends on whether the effect of long-range ion−DNA Coulomb interactions is ignored (the local binding model, LBM) or taken into account by stipulating that the total counterion concentration at the DNA surface is constant (the restricted polyelectrolyte model, RPEM). Although both models are approximate, the RPEM should be closer to reality. In the RPEM, a nonzero λ, and thus a reduction of β on Rb^+ addition, is obtained even if Rb^+ does not compete with Na^+ for the minor-groove site ($K_{Rb} = 0$ in eq 12). This is a consequence of the replacement of a fraction $C_{Rb}/(C_{Na} + C_{Rb})$ of the Na^+ ions at the surface by Rb^+ ions. Although the total ion concentration at the surface is constant in the RPEM, the surface concentration of Na^+ ions is reduced and therefore, by mass action, also the Na^+ occupancy ξ_{Na} in the minor groove decreases (if $K_{Rb} = 0$, some Na^+ ions are replaced by water molecules). In view of this ambiguity, the previous single-frequency competition data cannot be regarded as conclusive evidence of competitive ion binding in the minor groove. The interpretation is further complicated by the unresolved contributions from the β and γ dispersions to ΔR.

The new MRD data presented here improve the situation in two respects, thereby allowing us to resolve the competition issue. First, we have recorded the full ^{23}Na MRD profiles with and without added Rb^+ ions (Figure 2). With eqs 7 and 11, the β parameters derived from these dispersion profiles (Table 1) yield $\lambda = 1.8 \pm 0.5$. According to eq 12, the finding that $\lambda > 1$ implies, for both binding models, that $K_{Rb} > K_{Na}$. In other words, Rb^+ ions not only compete with Na^+ ions, but have a higher affinity than Na^+ ions for the minor groove. The second improvement is that we have now recorded the ^{87}Rb and ^{23}Na dispersions from the same mixed NaCl/RbCl sample (Figure 3). The observation of a pronounced ^{87}Rb β dispersion, which disappears on netropsin binding, is conclusive evidence of Rb^+ binding in the AT-tract of the minor groove. By comparing the β parameters from the ^{23}Na and ^{87}Rb dispersions recorded on the same sample, we can obtain the relative affinity of Na^+ and Rb^+ ions for the minor groove. According to eqs 7 and 10

$$\frac{K_{Rb}}{K_{Na}} = \left[\frac{\chi(^{23}Na)}{\chi(^{87}Rb)}\right]^2 \frac{\beta(^{87}Rb)}{\beta(^{23}Na)} \qquad (13)$$

This relation is valid for both binding models (RPEM and LBM) and does not require knowledge of the individual QCCs. If we assume, despite the larger size of the Rb^+ ion (crystal radius 1.5 Å, versus 1.0 Å for Na^+), that Na^+ and Rb^+ ions experience the same EFG when bound in the minor groove, then the QCC ratio in eq 13 is fully determined by the known nuclear quadrupole moments and electronic polarization factors, yielding $\chi(^{87}Rb)/\chi(^{23}Na) = 10.9$ (Section 2.5). With β parameters from Table 1, eq 13 thus yields $K_{Rb}/K_{Na} = 1.7 \pm 0.7$, indicating a similar, but slightly higher, affinity for Rb^+.

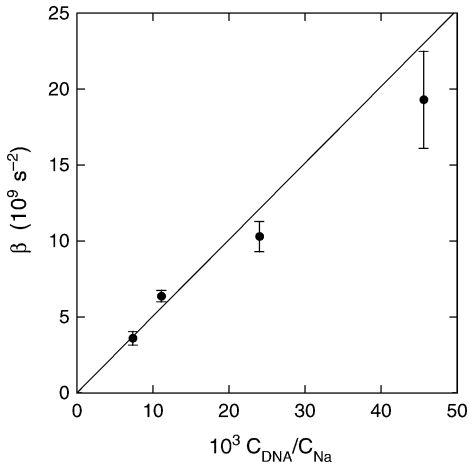

Figure 5. Variation of the ^{23}Na β dispersion amplitude with the duplex−DNA/Na^+ ratio. The solid line is a linear fit constrained to pass through the origin.

In conclusion, whether we compare the ^{23}Na dispersions with and without Rb^+ or the ^{23}Na and ^{87}Rb dispersions from the Na^+/Rb^+ sample, we arrive at the same conclusion: Rb^+ competes with Na^+ for binding in the minor groove and, in fact, has a slightly higher affinity than Na^+. This conclusion does not depend on the choice of binding model (LBM or RPEM).

4.2. Ion Occupancies. To obtain the absolute occupancies, ξ_{Na} and ξ_{Rb}, of ions bound in the minor groove, we need to know the QCCs $\chi(^{23}Na)$ and $\chi(^{87}Rb)$. On the basis of the calculations reported in Section 3.2, we adopt the values $\chi(^{23}Na) = 0.5$ MHz and $\chi(^{87}Rb) = 5.5$ MHz. It should be borne in mind that, since the occupancy derived from β scales as χ^{-2}, any systematic bias in χ is magnified in ξ. We consider first the Na^+ occupancy, ξ_{Na}^0, in the absence of Rb^+. In the RPEM, ξ_{Na}^0 is a constant, independent of C_{Na}. According to eqs 4 and 7

$$\beta = \left[\frac{2\pi^2}{5}\chi^2 \xi_{Na}^0\right]\frac{C_{DNA}}{C_{Na}} \qquad (14)$$

Table 1 contains four entries for samples with Na^+ as the only counterion (at 4 °C without netropsin). Figure 5 shows that the corresponding β values obey eq 14 within the experimental accuracy. The linear fit (forced to pass through the origin) yields a slope (the quantity within brackets in eq 14) of $(5.0 \pm 0.2) \times 10^{11}$ s^{-2}. With $\chi = 0.5$ MHz, this translates into $\xi_{Na}^0 = 0.51 \pm 0.02$. (Using only the β value obtained at $C_{DNA} = 1.5$ mM, rather than the slope in Figure 5, we obtain $\xi_{Na}^0 = 0.50 \pm 0.06$.) This is a considerably higher occupancy than deduced in the previous ^{23}Na MRD study.[8] The difference is mainly due to the larger QCC (1.3 MHz) used in the earlier study, based on crude EFG calculations with a short cutoff radius.

Having determined ξ_{Na}^0, we can use eqs 10−12 (for the RPEM) to calculate the variation in the Na^+ and Rb^+ occupancies as Rb^+ ions are added to the solution. For this calculation, we use the relative affinity, $K_{Rb}/K_{Na} = 1.74$, deduced from the ratio $\beta(^{87}Rb)/\beta(^{23}Na)$ (Section 4.1). Because the two ions have similar affinity for the minor groove, the total ion occupancy, $\xi_{Na} + \xi_{Rb}$, is insensitive to the bulk ionic composition (Figure 6). At the investigated composition (0.20 M Na^+, 0.56 M Rb^+),

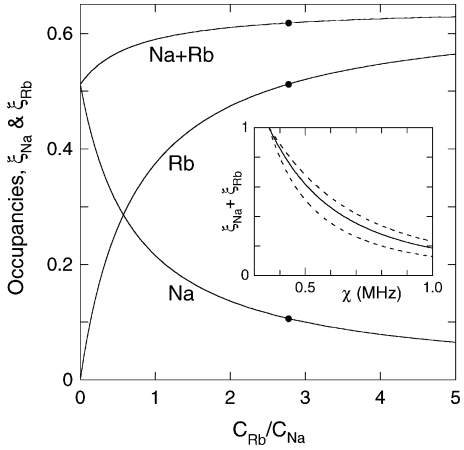

Figure 6. Variation of the Na^+ and Rb^+ occupancies in the minor groove with the overall ionic composition of the solution, as predicted by the RPEM with the ξ^0_{Na} and K_{Rb}/K_{Na} values deduced from the MRD data and $\chi = 0.5$ MHz. The dots refer to the composition of the investigated mixed-salt sample. The inset shows the dependence of the total ion occupancy on the ^{23}Na QCC, with $K_{Rb}/K_{Na} = 1.7 \pm 0.7$ (the dashed curves correspond to the error bounds).

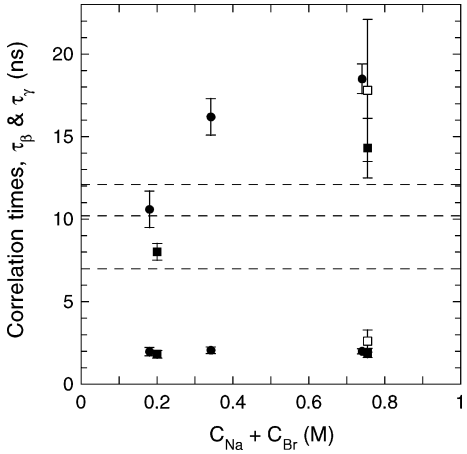

Figure 7. Correlation times τ_β and τ_γ (bottom, close to 2 ns) derived from ^{23}Na (solid symbols) or ^{87}Rb (open symbols) MRD data from 1.5 mM (squares) or 8.2 mM (circles) A_2T_2 solutions at 4 °C. The dashed lines represent the three rotational correlation times $\tau_R^{(M)}$, with $M = 0$, 1, and 2 from top to bottom, determined from ^{13}C relaxation[61] and scaled to 4 °C.

most of the Na^+ ions have been replaced by Rb^+ ions: $\xi_{Na} = 0.1$ and $\xi_{Rb} = 0.5$. The ion occupancies obtained directly from the β amplitudes in Table 1 with the aid of eqs 4 and 7 are $\xi_{Na} = 0.08 \pm 0.02$ and $\xi_{Rb} = 0.40 \pm 0.15$. The inset in Figure 6 shows how the total ion occupancy at this composition would change if we used a different QCC value (yielding a different ξ^0_{Na} by way of eq 14). For reasonable variations in χ, the occupancy remains substantial. As shown, the total occupancy is relatively insensitive to variations in K_{Rb}/K_{Na} within the error limits (1.0−2.4).

We use the RPEM rather than the LBM to derive absolute ion occupancies because, on theoretical grounds,[48−55] this is likely to be the more accurate of the two models. However, the MRD data per se do not allow us to discriminate between the models. Thus, within the experimental uncertainties, the data in Figure 5 are also consistent with the nonlinear dependence of β on $1/C_{Na}$ predicted by the LBM. (The nonlinear fit yields $\chi = 0.4 \pm 0.1$ MHz and $K_{Na} = 10 \pm 6$ M^{-1}.) Furthermore, the model-independent values of λ and K_{Rb}/K_{Na} obtained in Section 4.1 are mutually consistent within the framework of either binding model. With $K_{Rb}/K_{Na} = 1.7 \pm 0.7$ and $\xi^0_{Na} = 0.51 \pm 0.02$, eq 12 (for RPEM) yields $\lambda = 1.4 \pm 0.4$, which is consistent with the value, $\lambda = 1.8 \pm 0.5$, obtained directly from the ratio of the ^{23}Na β values measured with and without added Rb^+. This consistency provides additional support for our structure-based QCC calculations.

4.3. Exchange Kinetics. Orientational randomization of the EFG tensor experienced by a site-bound Na^+ or Rb^+ nucleus occurs by two independent processes: tumbling of the DNA duplex, with correlation time τ_R, and exchange of the ion from the binding site, with mean residence time τ_{res}. Accordingly, the observed correlation time, τ_β, can be expressed as[35]

$$\frac{1}{\tau_\beta} = \frac{1}{\tau_R} + \frac{1}{\tau_{res}} \qquad (15)$$

If $\tau_{res} \gg \tau_R$, we thus expect that $\tau_\beta = \tau_R$. On the other hand, if τ_β is found to be shorter than τ_R, then the difference allows us to estimate the residence time. To determine if this is the case, we need independent information about τ_R. A *B*-DNA dodecamer has an aspect ratio of about 2 and is therefore not expected to tumble as a spherical rotor. Hydrodynamic calculations indicate that the duplex is well described as a symmetric rotor, with the rotational diffusion coefficient, $D_{||}$, for rotation about the helix axis about twice as large as the rotational diffusion coefficient, $D_\perp$, for end-over-end tumbling.[59,60] Instead of a single tumbling time, τ_R, the SDF then involves a linear combination of three rotational correlation times, $\tau_R^{(M)} = [6D_\perp + M^2(D_{||} - D_\perp)]^{-1}$ with $M = 0$, 1 and 2. With $D_{||} = 2\ D_\perp$, the longest correlation time ($\tau_R^{(0)}$) exceeds the shortest one ($\tau_R^{(2)}$) by a factor 5/3. Because this difference is too small to be resolved in our MRD data, we describe the β dispersion with a single Lorentzian function (eq 2) and an effective rotational correlation time, τ_R. Knowing the orientation and asymmetry of the principal EFG tensor, we can relate τ_R to the three correlation times $\tau_R^{(M)}$. For our purposes, however, it suffices to know that $\tau_R^{(2)} \le \tau_R \le \tau_R^{(0)}$.

From ^{13}C R_1 and $R_{1\rho}$ relaxation measurements at 35 °C on the furanose carbons in the A_2T_2 dodecamer at 0.4 mM duplex in D_2O with 60 mM inorganic salt at pH 7.0, the rotational diffusion coefficients of the duplex have been deduced.[61] Scaling these (according to $D \sim T/\eta$) to the viscosity of D_2O at 4 °C, we obtain $D_{||} = 29\ (\mu s)^{-1}$ and $D_\perp = 14\ (\mu s)^{-1}$. In Figure 7, we compare the correlation times τ_β, derived from the ^{23}Na and ^{87}Rb dispersions (Table 1), with the three rotational correlation times $\tau_R^{(M)}$ obtained from ^{13}C relaxation. At a counterion concentration of 0.2 M, the MRD-derived τ_β is consistent with the independently determined $\tau_R^{(M)}$ values. From eq 15, we can therefore infer that $\tau_{res} > 10$ ns at 4 °C for Na^+ ions in the minor groove.

At higher counterion concentrations, the τ_β values lie in the range 14−18 ns (Figure 7), well above the rotational correlation times $\tau_R^{(M)}$ (7−12 ns) derived from ^{13}C relaxation[61] at lower salt concentration. This discrepancy indicates that the DNA duplex tumbles more slowly at high salt concentrations. In

(59) Fernandes, M. X.; Ortega, A.; López Martínez, M. C.; García de la Torre, J. *Nucl. Acids Res.* **2002**, *30*, 1782−1788.
(60) Ortega, A.; García de la Torre, J. *J. Chem. Phys.* **2003**, *119*, 9914−9919.
(61) Boisbouvier, J.; Wu, Z.; Ono, A.; Kainosho, M.; Bax, A. *J. Biomol. NMR* **2003**, *27*, 133−142.

contrast, depolarized light scattering measurements on a 20 base pair oligonucleotide at 20 °C indicated that the tumbling time decreases on addition of 100 mM NaCl.[62] To obtain an independent estimate of τ_R in the mixed-salt MRD sample at 4 °C, we performed ^{31}P relaxation measurements at two magnetic fields (Section 2.3). The longitudinal and transverse relaxation rates of the combined phosphodiester ^{31}P intensity were $R_1 = 0.467\ s^{-1}$ and $R_2 = 82.6\ s^{-1}$ at the lower field (corresponding to a ^{31}P resonance frequency of 202 MHz), and $R_1 = 0.508\ s^{-1}$ and $R_2 = 111\ s^{-1}$ at the higher field (243 MHz). At these high magnetic fields, the ^{31}P relaxation is strongly dominated by the chemical shielding anisotropy (CSA) mechanism, which causes the relaxation rates to increase with frequency.[31,32]

If the ^{31}P relaxation is governed entirely by the rotational diffusion of the DNA duplex, then τ_R can be extracted either from the ratio R_2/R_1 or from the difference $R_2 - 0.5\ R_1$ and the known[30] CSA parameters.[31] For our data, the former method yields $\tau_R = 12.8$ and 11.8 ns at the two frequencies, whereas the latter methods yields $\tau_R = 22.8$ and 21.2 ns. The factor-2 discrepancy indicates that the ^{31}P relaxation is affected by internal reorientational motions in the phosphodiester backbone. Recent ^{31}P MRD measurements on a DNA octamer have also shown that R_1 increases at high fields, as expected in the presence of internal motions.[63] Provided that the internal motions are of modest amplitude and are much faster than duplex tumbling, they should have little effect on the difference $R_2 - 0.5\ R_1$, which only involves the zero-frequency SDF. Hence, the longer τ_R values should be most accurate. This conclusion was confirmed by a global analysis of all four relaxation rates in terms of a SDF with two correlation times,[31] yielding a DNA tumbling time $\tau_R = 22 \pm 2$ ns, a local order parameter $S^2 = 0.9 \pm 0.1$, and an internal-motion correlation time $\tau_{int} = 0.7 \pm 0.2$ ns (Section 2.3).

The effective rotational correlation time τ_R is a function of the two rotational diffusion coefficients $D_{||}$ and $D_\perp$, but the form of this function depends on the orientation of the (locally averaged) CSA tensor (^{31}P), C−H vector (^{13}C) or EFG tensor (^{23}Na and ^{87}Rb). Not knowing these orientations, we conclude that the ^{23}Na and ^{87}Rb correlation times, $\tau_\beta = 14-18$ ns, obtained at high salt concentrations, are consistent with the ^{31}P correlation time, $\tau_R = 22$ ns. As in the low-salt case, we can then use eq 15 to establish that $\tau_{res} > 20$ ns for Na^+ and Rb^+ ions in the minor groove.

The physical origin of the salt-induced retardation of DNA tumbling is unclear at this stage and deserves further study. The salt effect on the bulk solvent viscosity is merely 2% for 0.2 M NaCl and even less after addition of 0.56 M RbCl.[64] A salt-dependent retardation could be produced by the finite response time of the counterion atmosphere in the time-dependent electric field of the rotating DNA duplex.[65−67] However, this electrolyte friction reduces the translational diffusion coefficient of oligonucleotides by at most 10%,[67] which is much less than the salt effect observed here. Moreover, electrolyte friction is predicted to be most important when the Debye length matches the radius of the double helix.[65−67] This corresponds to about 0.1 M, well below the range where τ_R is found to increase. Another mechanism of rotational retardation is the hydrodynamic interaction (HI), which becomes important on close approach of two macromolecules.[68] Because oligonucleotides are highly charged, they tend to be well separated and the relative rotational retardation due to HI should then be proportional to ϕ^2, where ϕ is the DNA volume fraction and the proportionality constant is close to 1.[69] At high salt concentrations, when the Coulomb repulsion is screened out, the ϕ dependence becomes first-order with the relative retardation equal to 0.67 ϕ (for hard spheres).[70] However, at a duplex concentration of 1.5 mM, ϕ is only 0.03 so that the HI effect is negligible.

Having excluded other mechanisms, we are left with orientation-dependent direct interactions between DNA duplexes. Such interactions can be of long range, involving the electric quadrupole moment of the duplex, or of short range, as in end-to-end stacking of two oligomers. The observed salt dependence rules out long-range electrostatic interactions, which should be most important at low salt concentrations. Hydrodynamic modeling shows that end-to-end dimerization of a dodecamer duplex decreases $D_\perp$ by a factor 4.1 and $D_{||}$ by a factor 1.7.[60] The observed effect could therefore be explained by partial self-association. In a fluorescence depolarization study of the A_2T_2 dodecamer, τ_R was found to increase by 40% when the duplex concentration was increased from 0.03 to 4 mM (in 0.2 M NaCl at 30 °C),[71] but a concentration dependence is not evident in our results (between 1.5 and 8.2 mM at 4 °C). However, depolarized light scattering studies of oligonucleotide rotation suggest that DNA−DNA interactions become more important at low temperatures.[72]

Information about the residence time is also provided by the fast-exchange condition, $\tau_{res} \ll (b\ \tau_R)^{-1}$. According to eqs 3 and 7, we have in the general case for ^{23}Na

$$\beta\tau_\beta = \frac{\xi_{Na} C_{DNA}}{C_{Na}} \frac{b\tau_R}{1 + b\tau_R\tau_{res}} \qquad (16)$$

In the fast-exchange limit, the temperature dependence of the product $\beta\ \tau_\beta$ is thus determined by $\xi_{Na}\ \tau_R$, whereas, in the opposite slow-exchange limit, it is determined by ξ_{Na}/τ_{res}. With $\chi(^{23}Na) = 0.5$ MHz and $\tau_R \approx 10$ ns (for 0.2 M NaCl), a slow-exchange situation would require $\tau_{res} > 0.1$ ms. If the residence time were as long as this, then it would presumably have a large activation enthalpy and a much stronger temperature dependence than ξ_{Na}. In the slow-exchange regime, we therefore expect $\beta\ \tau_\beta$ to increase at higher temperature. For the 1.5 mM A_2T_2 sample with 0.2 M NaCl (and no RbCl), we recorded the ^{23}Na MRD profile also at 27 °C (data not shown). As compared to 4 °C, the product $\beta\ \tau_\beta$ decreased by a factor 5 (Table 1), thus ruling out a slow-exchange situation. We conclude, therefore, that the Na^+ ions in the minor groove are in fast (or, possibly, intermediate) exchange with external ions, meaning that $\tau_{res} <$ 0.1 ms at 4 °C.

(62) Liu, H.; Skibinska, L.; Gapinski, J.; Patkowski, A.; Fischer, E. W.; Pecora, R. *J. Chem. Phys.* **1998**, *109*, 7556−7566.
(63) Redfield, A. G. *Magn. Reson. Chem.* **2003**, *41*, 753−768.
(64) Lide, D. R., ed. *Handbook of Chemistry and Physics*, 82nd ed.; CRC Press: Boca Raton, FL, 2001.
(65) Booth, F. *J. Chem. Phys.* **1954**, *22*, 1956−1968.
(66) Hernández-Contreras, M.; Alarcón-Waess, O.; Medina-Noyola, M. *J. Chem. Phys.* **1997**, *106*, 2492−2501.
(67) Allison, S.; Chen, C.; Stigter, D. *Biophys. J.* **2001**, *81*, 2558−2568.
(68) Happel, J.; Brenner, H. *Low Reynolds Number Hydrodynamics*; Nordhoff: Leyden, 1973.
(69) Hagen, M. H. J.; Frenkel, D.; Lowe, C. P. *Physica A* **1999**, *272*, 376−391.
(70) Jones, R. B. *Physica A* **1989**, *157*, 752−768.
(71) Nuutero, S.; Fujimoto, B. S.; Flynn, P. F.; Reid, B. R.; Ribeiro, N. S.; Schurr, J. M. *Biopolymers* **1994**, *34*, 463−480.
(72) Eimer, W.; Williamson, J. R.; Boxer, S. G.; Pecora, R. *Biochemistry* **1990**, *29*, 799−811.

In the case of ^{87}Rb, the QCC is an order of magnitude larger, making the fast-exchange condition (which involves χ^2) much more restrictive. With $\chi(^{87}\text{Rb}) = 5.5$ MHz and $\tau_R \approx 20$ ns, fast exchange thus requires that $\tau_{res} \ll 0.4$ μs. Because the fast-exchange regime only spans a factor 20 in τ_{res}, the ^{87}Rb MRD data (in the absence of netropsin) were analyzed with the general expressions (eq 3) that do not assume fast exchange. Although the data scatter prevents us from claiming a significant improvement in the quality of the fit (beyond that expected from introducing an additional parameter), the narrow range of the fast-exchange regime argues for the adopted procedure. The additional parameter is $b\tau_{res}$ (contained in the quantity ϵ in eq 3), which, for $\chi(^{87}\text{Rb}) = 5.5$ MHz, yields $\tau_{res} = 0.2 \pm 0.1$ μs for Rb^+ ions in the minor groove at 4 °C. We are thus on the "fast" side of the intermediate-exhange regime, with the β dispersion step (given by β τ_β) reduced by about 30% as compared to fast-exchange conditions.

4.4. Structural Dependence of QCCs. The ion occupancy derived from MRD data depends quadratically on the QCC. It is therefore important to estimate the QCC as accurately as possible. Our EFG calculations are based on structures of the A_2T_2 duplex determined by cryocrystallography.[4,22,47] Crystal packing interactions, the presence of spermine, Mg^{2+} ions and organic cosolvent (MPD), and the low temperature (120−175 K) could all cause the solvated DNA structure to differ from that in our solutions. Indeed, the NMR-derived room-temperature solution structure of the A_2T_2 duplex differs significantly from the crystal structure, particularly in the GC flanks.[73] However, the EFG is mainly affected by the local structure in the AT-tract, which appears to be quite robust, with only 0.6 Å RMSD between crystal and solution structures of the six central base pairs.[73]

The EFG at the Na^+ or Rb^+ nuclear site depends sensitively on the local coordination geometry, including the position and orientation of first-shell water molecules. The three A_2T_2 structures used in our EFG calculations were determined from crystals grown with Na^+, K^+, or Rb^+ as the only monovalent counterion in the mother liquor.[4,22,47] In one of these structures (460d), a Rb^+ ion was modeled with 50% occupancy in the ApT site.[4] Whether Na^+ or K^+ ions penetrate the minor groove in the other structures is unclear, because of the difficulty of distinguishing the lighter alkali ions from water molecules in the electron density map.[20] The primary coordination of the ApT solvent site is very similar in the three structures, with two thymine O2 atoms and two water oxygens (in the secondary solvation layer) at a distance of 2.8 ± 0.1 Å (Table 3). In addition, there are two furanose O4′ atoms at 3.4 ± 0.1 Å. It thus appears that Rb^+ binds to the ApT site with little or no change in coordination geometry. This is not surprising, since both Rb^+ and water prefer to have oxygen ligands at a distance of 2.8 Å.[74] Our calculations should therefore be regarded as giving the EFG experienced by a Rb^+ ion in the ApT site. Consequently, the Rb^+ occupancy derived from the MRD data with the aid of the calculated QCC should be more reliable than the Na^+ occupancy.

In our analysis of the MRD data, we have assumed that a Na^+ ion in the ApT site experiences the same EFG as a Rb^+ ion in the same site. Since the preferred Na^+−O distance is 2.4 Å (rather than 2.8 Å),[74] a Na^+ ion in the ApT site might alter the local structure to some extent. (If this is the case, the observed 2.8 Å coordination of the ApT site in the Na^+-containing crystal 436d rules out a high Na^+ occupancy.) The calculated QCC, $\chi(^{23}\text{Na}) = 0.5$ MHz, is smaller than the QCCs that have been determined by solid-state NMR for Na^+ complexes with crown ethers, cryptands and ionophores,[75] for oxygen-coordinated Na^+ in inorganic crystals,[76] and for Na^+ in mononucleotide crystals.[77,78] In most of these cases, $\chi(^{23}\text{Na})$ is in the range 1−3 MHz and the Na^+−O distances are generally close to 2.4 Å. The EFG depends not only the number of ligands and their separation; it also depends on the coordination symmetry. In fact, the EFG vanishes for regular tetrahedral, octahedral or cubic coordination. In the ApT site, the primary (2.8 Å) coordination is not far from tetrahedral and this is likely to be the main reason for the unusually small EFG. In most cases examined by solid-state NMR, crystal packing constraints tend to distort the coordination geometry from the preferred unconstrained high-symmetry situation.

We have performed EFG calculations, with the same protocol as used here for A_2T_2, for the four internal Na^+ ions in the dimeric foldback quadruplex of the dodecamer $d(G_4T_4G_4)$.[79,80] As compared to the ApT site in the A_2T_2 duplex, these ions have higher coordination, with 7 or 8 oxygen atoms at separations of 2.1−3.3 Å and adjacent Na^+ ions at about 4 Å. For these less symmetric sites, we obtain larger QCCs of 1.0−1.8 MHz, in the same range as determined by solid-state NMR for a synthetic guanosine quadruplex (1.5−1.8 MHz).[81]

We have also performed EFG calculations as a function of ion position near the ApT site in the A_2T_2 structure 460d. These calculations show that the crystallographic Rb^+ site is within 0.1 Å of the minimum of the EFG surface, as expected for a symmetric coordination. Any contraction of the coordination or thermal averaging of the structure should therefore increase the effective QCC. With a larger ^{23}Na QCC, the MRD data would yield a smaller Na^+ occupancy and a higher ion selectivity (larger K_{Rb}/K_{Na}). Simulation-based EFG calculations might shed further light on these issues, provided that the force field can accurately model the thermodynamics of partial dehydration of ions in the minor groove. This is unlikely, however, since the experimentally established partial occupancy implies that the free energy difference between free and bound ions is merely a few kJ mol^{-1}.

4.5. Location of the Binding Site. The MRD data presented here and in our previous study[8] demonstrate that the long-lived ions, responsible for the low-frequency β dispersion, are located in the AT tract of the minor groove. This conclusion follows from the observation that binding of netropsin (to the AT tract) abolishes the β dispersion (Figures 2 and 3) and from the finding[8] that the amplitude of the β dispersion correlates with the nucleotide base sequence (the length of the AT tract). But the MRD data do not pinpoint the ion location within the rather

(73) Wu, Z.; Delaglio, F.; Tjandra, N.; Zhurkin, V. B.; Bax, A. *J. Biomol. NMR* **2003**, *26*, 297−315.
(74) Dobler, M. *Ionophores and Their Structures*; Wiley: New York, 1981.
(75) Wong, A.; Wu, G. *J. Phys. Chem. A* **2000**, *104*, 11 844−11 852.
(76) Koller, H.; Engelhardt, G.; Kentgens, A. P. M.; Sauer, J. *J. Phys. Chem.* **1994**, *98*, 1544−1551.
(77) Ding, S.; McDowell, C. A. *Chem. Phys. Lett.* **2000**, *320*, 316−322.
(78) Wong, A.; Wu, G. *J. Phys. Chem. A* **2003**, *107*, 579−586.
(79) Horvath, M. P.; Schultz, S. C. *J. Mol. Biol.* **2001**, *310*, 367−377.
(80) Schultze, P.; Smith, F. W.; Feigon, J. *Structure* **1994**, *2*, 221−233.
(81) Wong, A.; Fettinger, J. C.; Forman, S. L.; Davis, J. T.; Wu, G. *J. Am. Chem. Soc.* **2002**, *124*, 742−743.

large volume excluded (or perturbed) by the netropsin molecule. In calculating the QCC, required to obtain the absolute ion occuancy, we have assumed that the ion is located at one of the primary solvation sites, where it interacts directly with the polar atoms of the nucleotide bases. However, the netropsin molecule also displaces the secondary and tertiary solvation layers in the AT tract of the minor groove, so it might be argued that the long-lived ions do not penetrate deeply into the groove. Nevertheless, the available structural, thermodynamic, and kinetic data argue strongly for direct ion coordination to the nucleotide bases at the floor of the groove. The arguments are as follows.

A fully hydrated Rb^+ ion (with its first hydration shell) has a van der Waals radius of about 8.4 Å, whereas the narrow minor groove of the AT tract has a width of 4.0 ± 0.5 Å (measured either as the cross-strand P−P separation less 5.8 Å or the cross-strand O4′−O4′ separation less 2.8 Å). The ion must therefore be partly dehydrated before it can enter the minor groove. Because of the very large dehydration energy (see below), this structural constraint effectively prevents ions from accessing the minor groove unless polar DNA atoms can replace the lost water molecules in the coordination shell of the ion. This is possible for the primary solvation sites at the floor of the groove, where thymine O2, adenine N3, and furanose O4′ atoms are available. In contrast, for the secondary solvation sites, there are no polar DNA atoms within 3.5 Å (the closest being O4′ at about 4 Å). For the tertiary solvation sites, oxygen atoms in the phosphodiester groups can serve as ion ligands, but the exposed ion location at the lips of the minor groove is not compatible with the long residence time (0.2 μs for Rb^+), which indicates a deeply buried binding site. According to MD simulations, Na^+ ions in such phosphate-bridging locations exchange on the 1−2 ns time scale.[12] We therefore believe that such phosphate-bridging ions are responsible for the γ dispersion, with a 2 ns correlation time (Table 1), rather than for the β dispersion. This assignment is further supported by the finding that the γ dispersion remains, albeit with reduced amplitude, when the AT-tract is blocked by netropsin (Table 1).

In analyzing the MRD data, we have assumed that each duplex contains a single site, where ions can bind with sufficiently long residence time to contribute to the β dispersion. The fact that we obtain occupancies less than unity is consistent with this assumption. While the simultaneous binding of two ions in the AT-tract of the minor groove is highly unlikely for electrostatic reasons, ions might alternate between different binding sites within groove. However, several lines of evidence point to the ApT site as the dominant ion binding site within the minor groove. First, this is the only site where the nucleotide bases provide two oxygen ligands, which, on account of their higher electronegativity, are preferable to nitrogen as alkali cation ligands. Second, electrostatic calculations indicate that the ApT site has a more negative electric potential than the flanking ApA sites.[9,82] Third, the only firm crystallographic evidence for alkali ions in the minor groove of A_2T_2 locates them exclusively (Rb^+) or predominantly (Cs^+) at the ApT site.[4,5] During the exchange process, the ion must transiently occupy other sites in the minor groove. However, if the duration of the exchange event is much shorter than the residence time in the ApT site (as seems likely), then the transiently populated sites will not contribute significantly to the equilibrium ion distribution that controls the β parameter. Furthermore, ion exchange is likely to be a highly cooperative process, involving the simultaneous movement of the ion and the surrounding water molecules in a transiently widened groove. The residence time of the ordered water molecules in the minor groove AT-tract of A_2T_2 is 1 ns at 4 °C (in the absence of added salt),[83] 200-fold shorter than the Rb^+ residence time determined here. Some or all of the Rb^+-coordinated water molecules in the minor groove may well have longer residence times. This could be checked by ^{17}O MRD measurements in the presence of Rb^+ ions.

4.6. Thermodynamics of Ion Binding. Information about the thermodynamics of Na^+ binding in the minor groove can be obtained from temperature-dependent MRD data. For one of our samples, with 0.2 M Na^+ and no Rb^+, ^{23}Na MRD profiles were recorded at 27 °C as well as at 4 °C. Because the correlation times are shorter at 27 °C, the parameters of the β and γ dispersions could not be determined with useful accuracy from an unconstrained bi-Lorentzian fit. We therefore fixed τ_β to the DNA tumbling time, $\tau_R = 3.7$ ns, obtained by η/T scaling of τ_β from 4 to 27 °C. If the QCC is constant (as expected), the temperature dependence in β is entirely due to the ion occupancy, ξ^0_{Na}. From the ratio of the β parameters determined at the two temperatures (Table 1), we thus obtain $\xi^0_{Na}(27\ °C)/\xi^0_{Na}(4\ °C) = 0.4 \pm 0.1$. This result is independent of the QCC value. The finding that $\xi^0_{Na}(27\ °C) < \xi^0_{Na}(4\ °C)$ demonstrates that Na^+ binding to the minor groove is associated with an enthalpy decrease. This is a nontrivial result, because Na^+ binding could have been driven by an entropically favorable release of first-shell hydration water to the bulk, despite an unfavorable enthalpy change.

All the recent high-resolution crystal structures of the A_2T_2 duplex have been determined after flash-cooling the crystal to low temperature (<200 K). With typical crystal sizes and cooling protocols, it takes 10−100 ms to reach the glass transition temperature of ca. 200 K, where diffusive motions are quenched.[24,84] For the residence times deduced here (0.2 μs for Rb^+ at 4 °C), the exchange kinetics are sufficiently fast to maintain the equilibrium Boltzmann populations during the cooling process.[24] The investigated crystals therefore have equilibrium ion occupancies corresponding to a temperature near 200 K. If the binding enthalpy is negative, as indicated by the temperature dependence of the MRD data, the ion occupancy should be considerably higher in the crystal than in solution (at 4 °C). Given that $\xi_{Rb} = 0.4$ at 4 °C, as deduced from the ^{87}Rb MRD data, we expect the binding site to be saturated in the crystal. Yet, in the Rb^+-containing crystal structure 460d, the ApT site was modeled with $\xi_{Rb} \approx 0.5$.[4] The close agreement of the crystal and solution occupancies must be coincidental. In the crystal, the low temperature would make $\xi_{Rb} = 1$, but other factors work in the opposite direction. Chief among these is the ionic composition of the solvent. In the MRD sample, 0.56 M Rb^+ ions are competing with 0.2 M Na^+ ions and 55 M water molecules for the ApT site. The crystal was grown from a solution with a DNA concentration similar to ours, but with 20 mM Rb^+, 25 mM Mg^{2+}, 3 mM spermine, and 40%

(82) Lavery, R.; Pullman, B. *J. Biomol. Struct. Dyn.* **1985**, *5*, 1021−1032.
(83) Denisov, V. P.; Carlström, G.; Venu, K.; Halle, B. *J. Mol. Biol.* **1997**, *268*, 118−136.
(84) Kriminski, S.; Kazmierczak, M.; Thorne, R. E. *Acta Crystallogr. D* **2003**, *59*, 697−708.

MPD.[3] However, the ion and solvent composition inside the crystal is unknown. While 22 units of counterion charge per duplex are required for electroneutrality, only 3.5 units were localized.[3]

Our result, $K_{Rb}/K_{Na} = 1.7$, for the ion selectivity of the ApT site is based on eq 10, which assumes that the bound ions are in equilibrium with a reservoir of a free ions with the same Rb^+/Na^+ ratio as in the bulk solution. However, the higher Rb^+ occupancy may be due, at least in part, to a preferential accumulation of Rb^+ ions (at the expense of Na^+ ions) at the DNA surface (including phosphate-bridging locations). In principle, information about the surface concentration of ions is contained in the α and γ amplitudes (Table 1), but the quantitative analysis of these parameters is highly model-dependent.[85]

The ion selectivity deduced from our MRD data, $K_{Rb}/K_{Na} = 1.7$, corresponds to a standard free energy, $\Delta G°(Na^+ \rightarrow Rb^+) = -1.3$ kJ mol^{-1}, for the replacement of Na^+ by Rb^+ in the minor groove site. This free energy difference may be decomposed as

$$\Delta G° (Na^+ \rightarrow Rb^+) = \Delta\Delta G°_{DNA} - \Delta\Delta G°_{hyd} \qquad (17)$$

where $\Delta\Delta G°_{DNA} = \Delta G°_{DNA,Na} - \Delta G°_{DNA,Rb}$ is the difference in interaction free energy of the two ions in the minor-groove binding site and $\Delta\Delta G°_{hyd} = \Delta G°_{hyd,Na} - \Delta G°_{hyd,Rb}$ is the difference in hydration free energy. The latter quantity has been determined experimentally:[86] $\Delta\Delta G°_{hyd} = -95$ kJ mol^{-1}. From eq 17, we can thus infer that $\Delta\Delta G°_{DNA} = -96.3$ kJ mol^{-1}. The large difference in hydration free energy is thus nearly (to within 1.4%) balanced by an equally large difference in binding free energy. This means that the environment of the bound ion in the minor groove is nearly as polarizable as bulk water. In other words, the weak observed ion selectivity implies that the cation binding site in the minor groove has sufficient flexibility to provide nearly the same stabilization for ions of different size. This is made possible by the two primary water ligands (Table 3) and by the flexible groove width.[10−14] Although the weak ion selectivity observed here is consistent with the previously discussed "flexible ionophore" picture of the minor groove,[16] our results do not provide evidence for or against an ion-induced groove narrowing.

The weak Rb^+/Na^+ selectivity deduced here for the ApT site in the minor groove contrasts with the much higher K^+/Na^+ selectivity exhibited by the internal sites in quadruplex DNA[87−89] and by ion channel proteins.[90,91] The high selectivity of those binding sites is a consequence of more rigid structural constraints. In the case of quadruplex DNA, selectivity is further enhanced by the complete dehydration of the bound ions.

5. Conclusions

By performing ^{23}Na and ^{87}Rb MRD measurements on the same mixed-salt solution, we have obtained direct evidence for long-lived and competitive binding of Rb^+ and Na^+ ions to the A_2T_2 dodecamer in solution. By blocking the AT-tract of the minor groove with netropsin, we have demonstrated that the long-lived ions are located in this region, most likely in the central ApT site at the floor of the minor groove. At 4 °C, the mean residence time is 0.2 ± 0.1 μs for Rb^+ and in the range 10 ns to 100 μs for Na^+. It should be understood that the numbers quoted for Na^+ refer to lower and upper bounds, rather than to ranges of observed residence times.

Quantitative estimates of ion occupancies can only be obtained from MRD data if the QCCs are known. From EFG calculations on crystal structures, we obtained $\chi(^{23}Na) = 0.5$ MHz and $\chi(^{87}Rb) = 5.5$ MHz. Because the crystallographic coordination geometry of the ApT site is closer to what is expected for a bound Rb^+ ion than for a Na^+ ion, the QCC estimate for ^{87}Rb should be more accurate. For a solution with 0.56 M Rb^+ and 0.20 M Na^+, this QCC value yields a 40% Rb^+ occupancy in the ApT site. Assuming that the bound Na^+ ion experiences the same EFG as the Rb^+ ion, we obtain a 10% Na^+ occupancy in the same solution, increasing to 50% in the absence of Rb^+ ions. These occupancies suggest that groove-bound alkali ions can play a significant role in the structural polymorphism of DNA in vivo. The ApT site is found to have a slight preference for Rb^+ ions, with a relative affinity, $K_{Rb}/K_{Na} = 1.7 \pm 0.7$, that may be partly due to preferential accumulation of Rb^+ ions near the phosphate groups at the lips of the minor groove. The 2 ns correlation time observed in all MRD profiles is tentatively assigned to counterions bridging cross-strand phosphate groups.

Acknowledgment. We thank Maurice Guéron for a stimulating dialogue and Bengt Jönsson for helpful discussions. This work was supported by the Swedish Research Council.

JA049930Z

(85) Halle, B. *Mol. Phys.* **1987**, *60*, 319−370.
(86) Schmid, R.; Miah, A. M.; Sapunov, V. N. *Phys. Chem. Chem. Phys.* **2000**, *2*, 97−102.
(87) Williamson, J. R. *Annu. Rev. Biophys. Biomol. Struct.* **1994**, 703−730.
(88) Hud, N. V.; Smith, F. W.; Anet, F. A. L.; Feigon, J. *Biochemistry* **1996**, *35*, 15 383−15 390.
(89) Wong, A.; Wu, G. *J. Am. Chem. Soc.* **2003**, *125*, 13 895−13 905.
(90) Hille, B. *Ionic Channels of Excitable Membranes*, 2nd Ed.; Sinauer: Sunderland, MA, 1992.
(91) Doyle, D. A.; Cabral, J. M.; Pfuetzner, R. A.; Kuo, A.; Gulbis, J. M.; Cohen, S. L.; Chait, B. T.; MacKinnon, R. *Science* **1998**, *280*, 69−77.